Accretion Growth History of SMBHs

Masayuki Akiyama

2015/11/13

Comparison of AGN (X-ray) Luminosity Functions

- Comparison of cosmological evolution of hard X-ray AGN luminosity functions determined from different X-ray surveys. Except for the z>5 estimates, the derived luminosity functions match sufficiently well each other (need to note: samples are not fully independent).

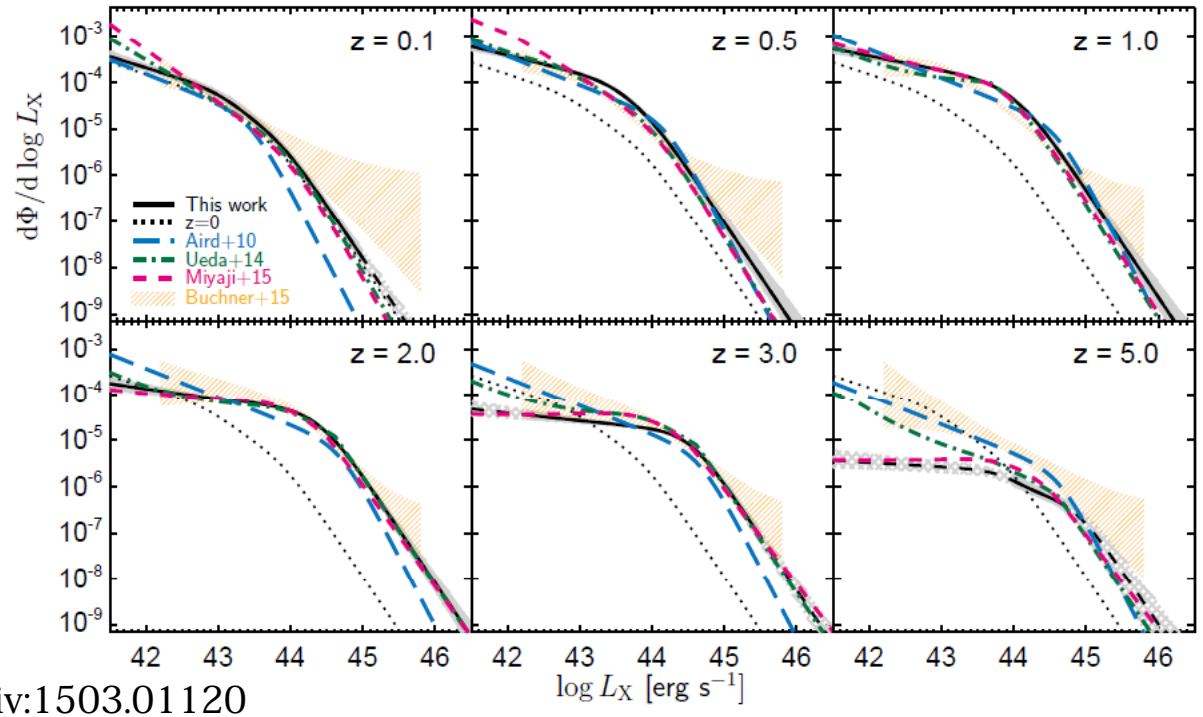

Aird et al. 2015, arXiv:1503.01120

Figure 12. Our model for the total XLF of all Compton-thin ($N_H < 10^{24}$ cm^{-2}) AGNs (black solid line, grey region indicates 99 per cent confidence interval in model parameters, dashed line and grey hatching indicate where we lack data and are extrapolating our model) compared to prior model fits: the LADE model from Aird et al. (2010, blue long-dashed line); the LDDE2 model from Ueda et al. (2014, green dot-dashed line); and the LDDE model from Miyaji et al. (2015, pink short-dashed line). We also show estimates from Buchner et al. (2015) who used a non-parametric method with simple smoothness assumptions to estimate the space density in fixed bins of L_X, N_H and z (orange hatched region indicate their 90 per cent confidence intervals for bins that approximately span the indicated redshift and include all Compton-thin AGNs).

Cosmological evolution of accretion density in the universe

- Cosmological evolution of AGN bolometric luminosity density in the unit co-moving volume

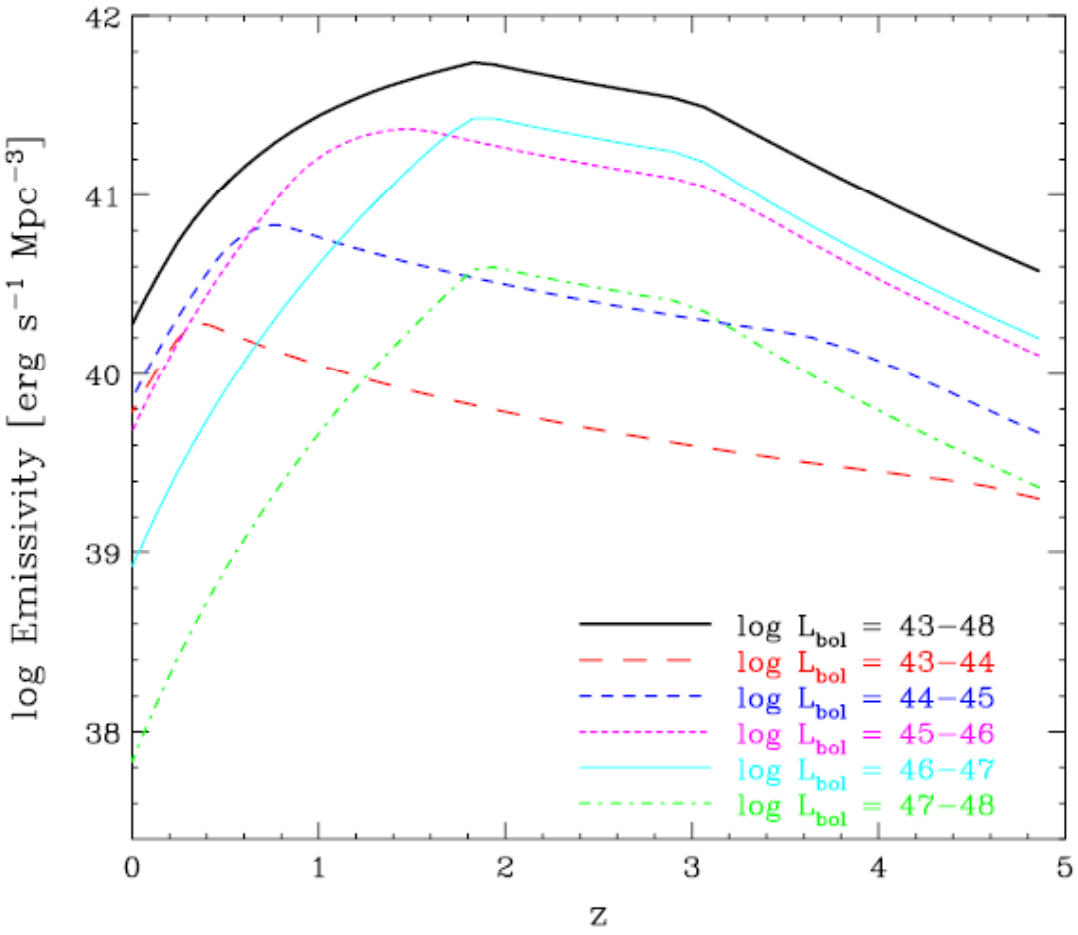

Ueda, MA et al. 2014

Accretion history of SMBHs and SF history of galaxies

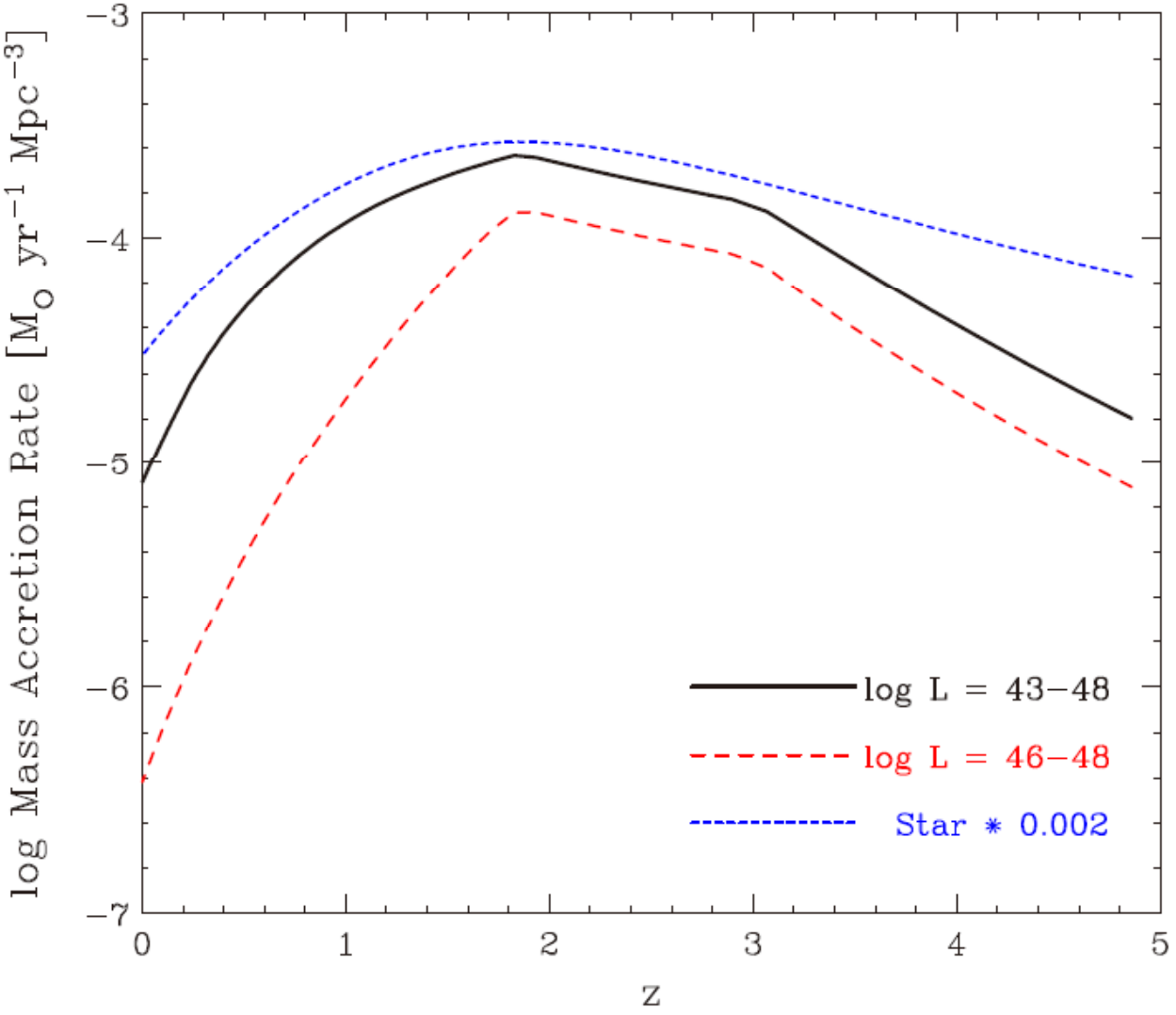

Ueda 2015

AGN accretion

Ueda, MA, et al, 2014, ApJ, 786, 104

SFR density

Madau&Dickinson 2014 ARAA, 52, 415

Accumulation of AGN “relic”

- Redshift evolution of black hole mass density determined with constant radiation efficiency of 0.05, which corresponds to non-spinning black hole.

Range of estimated local mass density of SMBHs. Systematic uncertainty associated with MBH-Mbulge relation affects the estimate.

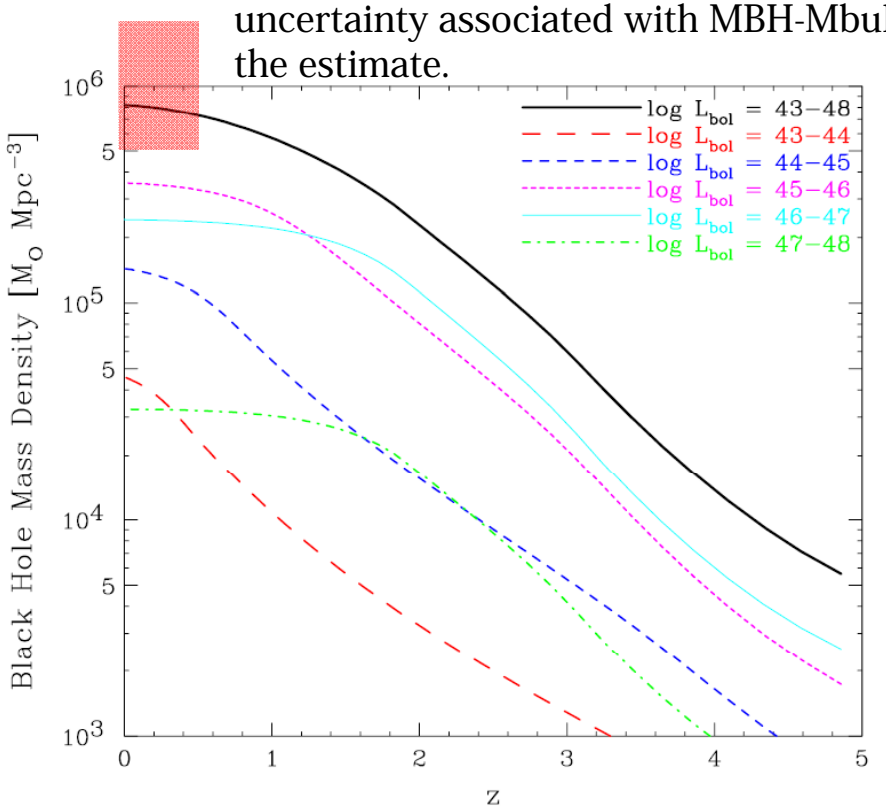

Figure 21. Comoving mass density of all SMBHs plotted against redshift (uppermost solid curve, black). Those calculated within limited luminosity ranges are separately shown. The averaged radiation efficiency of $\overline{\eta} = 0.05$ is assumed.

Ueda, MA et al. 2014

Constraints on the "typical" Eddington ratio and radiation efficiency

- Comparing AGN "relic" mass function of SMBHs with local mass function of SMBHs, the typical Eddington ratio of during accretion growth can be constrained.

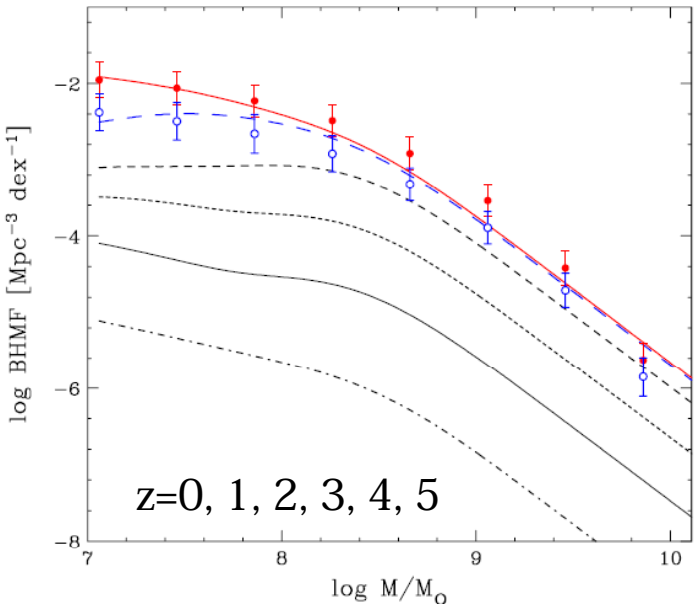

Ueda, MA et al. 2014

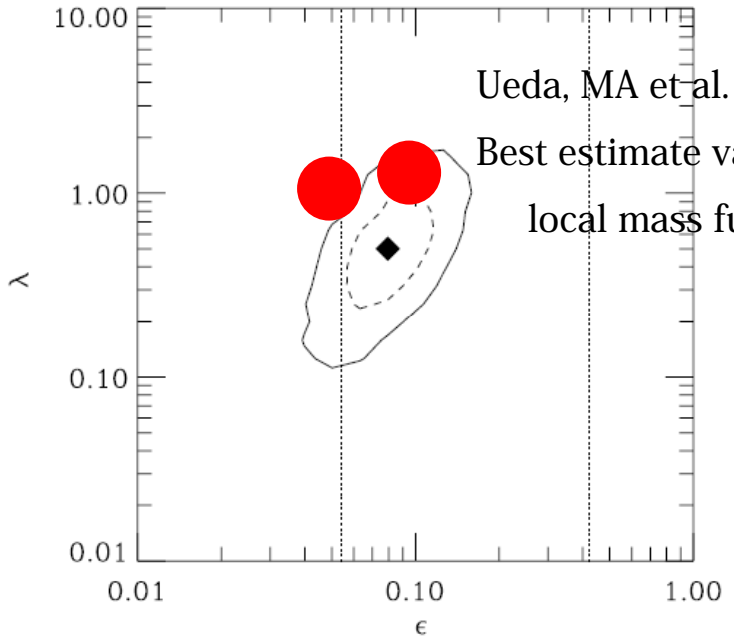

Ueda, MA et al. 2014

Best estimate vary depending on local mass function

Figure 7. Locus where accretion efficiency ε and Eddington ratio λ provide the best match between the local and relic BHMFs. The solid and dashed lines limit the regions where the logarithms of the local and relic BHMF differ, on average, by less than 1σ and 0.7σ (see text). The filled diamond marks the k^2 minimum and corresponds to $\varepsilon = 0.08$ and $\lambda = 0.5$. The cross indicates $\varepsilon = 0.1$ and $\lambda = 1$. The dashed lines are theoretical efficiencies for non-rotating ($\varepsilon = 0.054$) and maximally rotating BHs ($\varepsilon = 0.42$).

Original: Marconi et al. 2004, MNRAS, 351, 169

Eddington ratio distribution function determined with the X-ray-selected broad-line AGNs

- In reality, even within a relatively narrow luminosity range (~1dex), AGNs have wider range of Eddington ratio (~2dex).

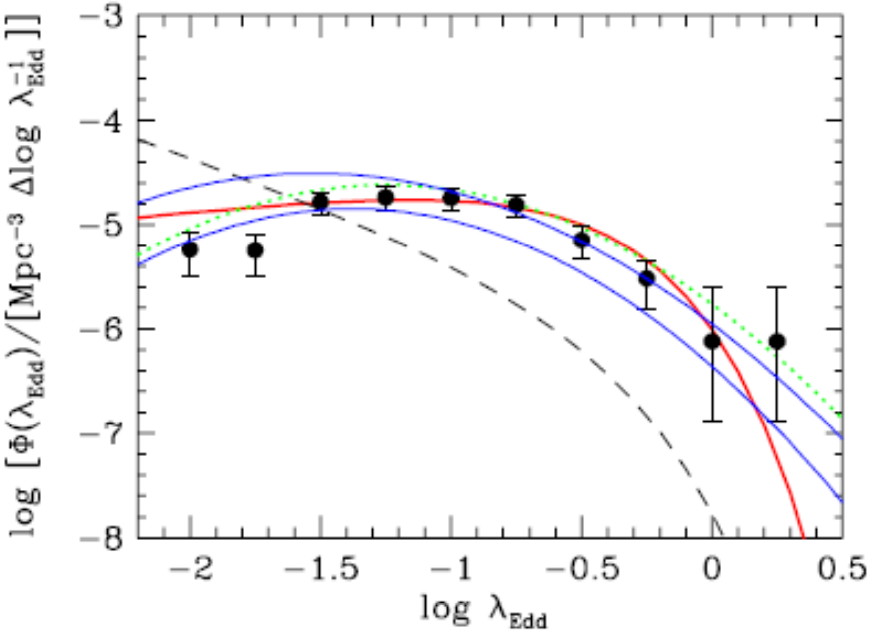

Figure 16. Binned (filled circles) and corrected broad-line AGN ERDF (thick solid line with Schecheter ERDF and thick dotted line with log-normal ERDF) from SXDS compared with the estimated broad-line AGN ERDF at $z \sim 1.4$ from SDSS (Shen & Kelly 2012; thin solid lines). The upper and lower thin solid lines represent the 68% enclosed region. The thin dashed line shows the corrected broad-line AGN ERDF in the local universe from Schulze & Wisotzki (2010).

Eddington ratio distribution function determined with z=1.2-1.7 broad-line AGNs found in the Subaru XMM-Newton Deep Survey.

Nobuta, MA, et al, 2012, ApJ, 761, 143

ERDF of broad-line AGNs

- Once the SDSS AGNs are combined, the range of the Eddington ratio can be wider.

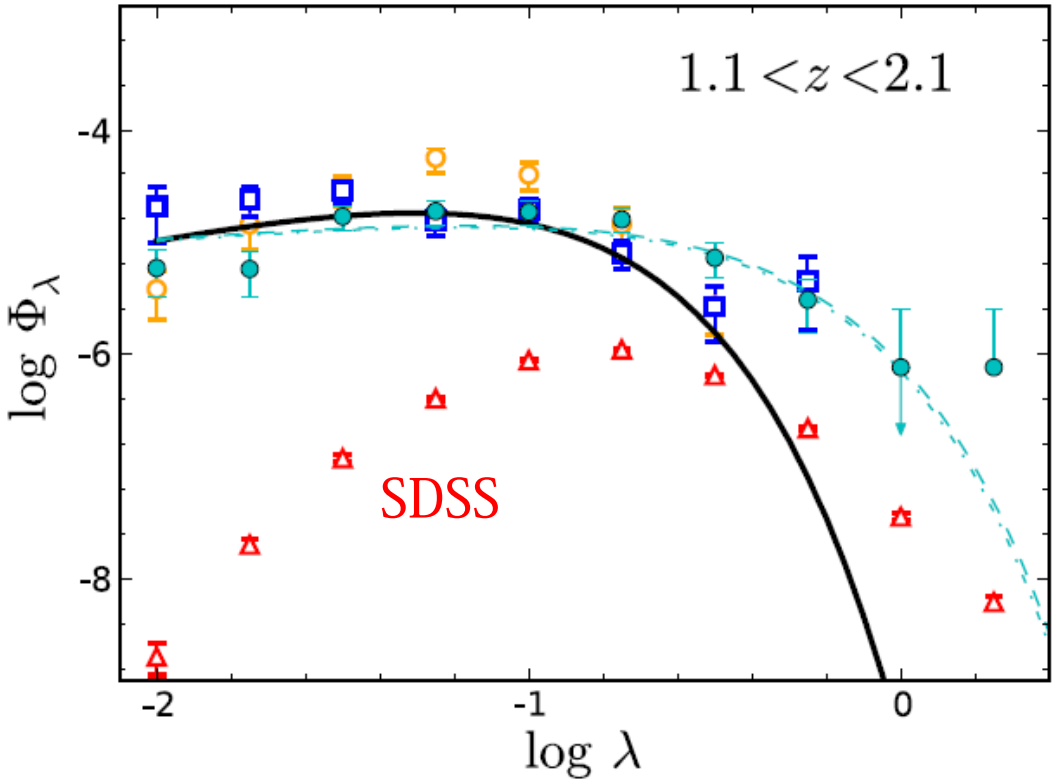

Recent update on broad-line AGN BHMF and ERDF with SDSS/VVDS/COSMOS AGNs

Schulze et al. 2015, MNRAS, 447, 2085

"*De-convolving*" AGN LF

- In order to understand what drives the cosmological evolution of AGN LF, we need to "de-convolve" AGN LF into BHMF and ERDF.

- BHMF ⊗ ERDF = AGN LF

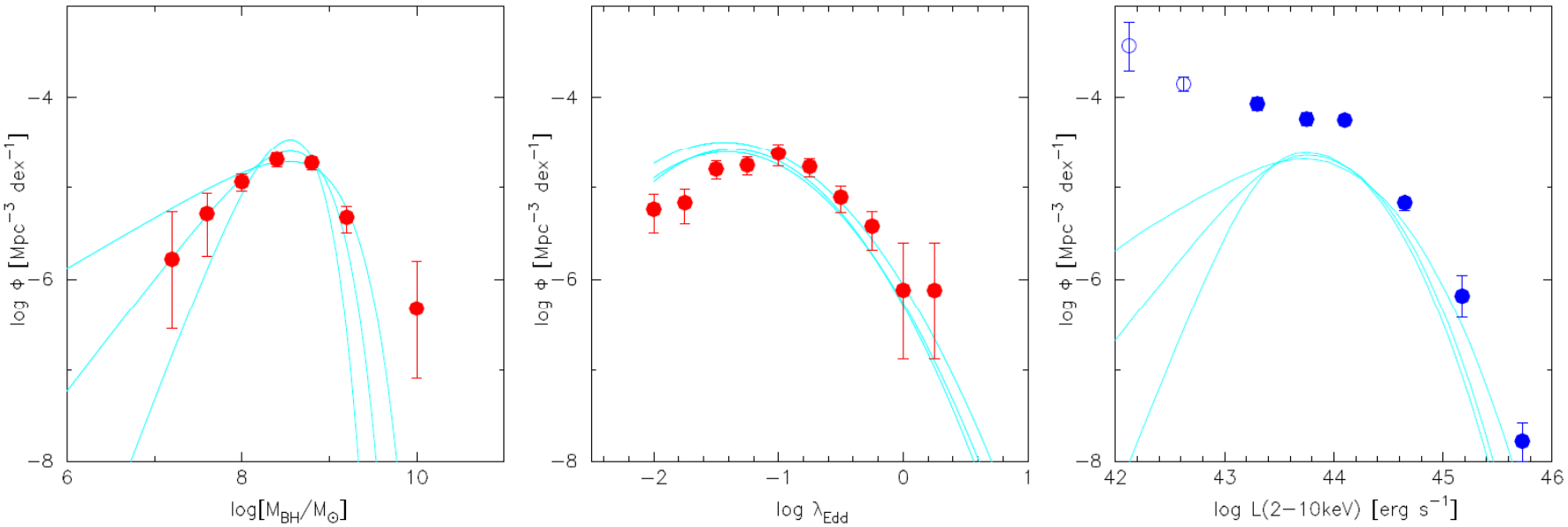

Convolution of BHMF and ERDF of X-ray-selected broad-line AGNs at z=0.6-2.0 compared with X-ray LF in the same redshift range.

“De-convolving” AGN LF

- Further more, contribution from obscured narrow-line AGNs needs to be included to understand the BHMF in the low mass range and the “meaning” of the AGN LF.
- BHMF ⊗ ERDF = AGN LF

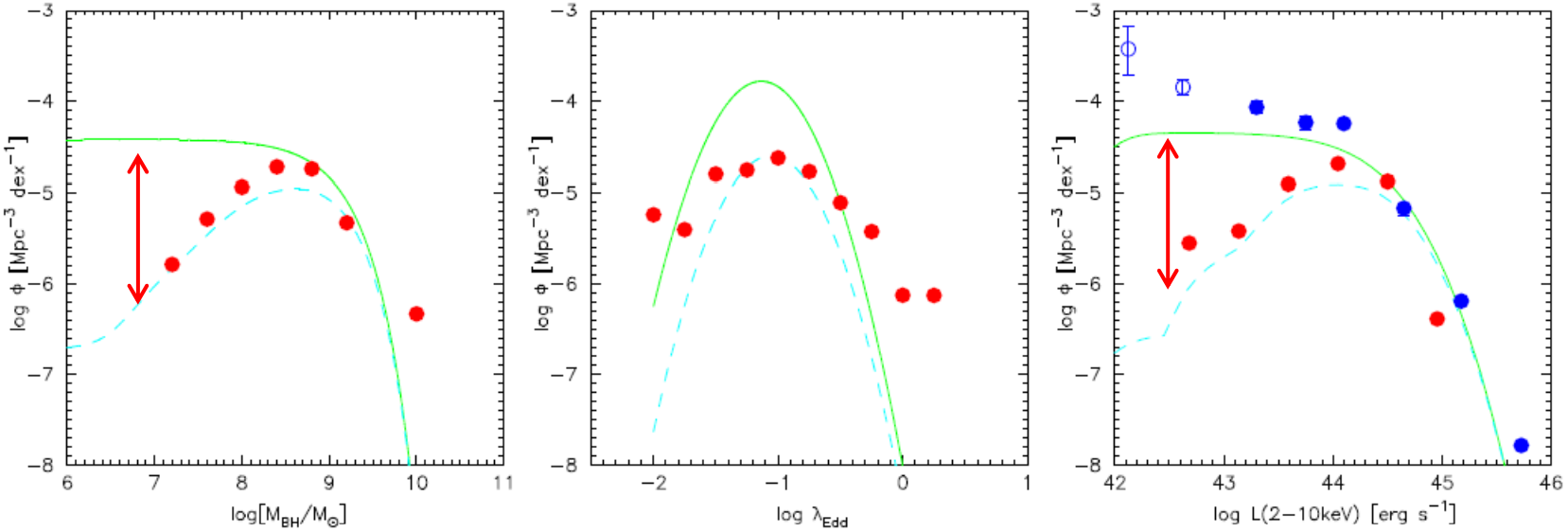

↕ Represents to estimated contribution from obscured AGN

Current sample size is limited at 8-10m spectroscopy limit

- Large number of QSO spectra is available at SDSS limit, but they are mostly high mass (>10^9 Msolar) and high Eddington (~1) AGNs. We need samples at 8-10m spectroscopy limit in order to unveil the majority of the AGN population (major part of the accretion growth of SMBHs).

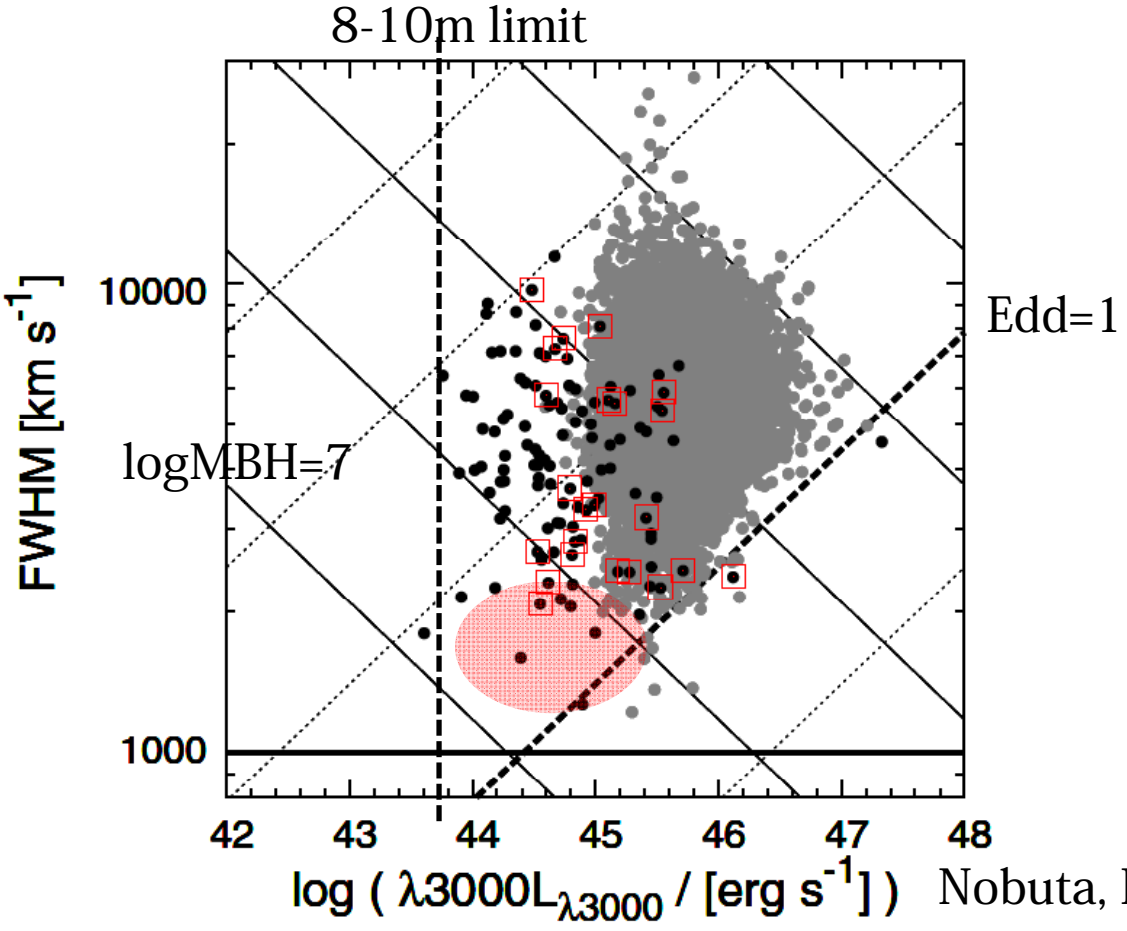

Nobuta, MA, et al, 2012

Combination with “galaxy” sample is important

- “galaxy” sample is unique to pick out Compton-thick AGN candidates, which are largely missed in the current X-ray samples.

Compton-thin: X-ray select

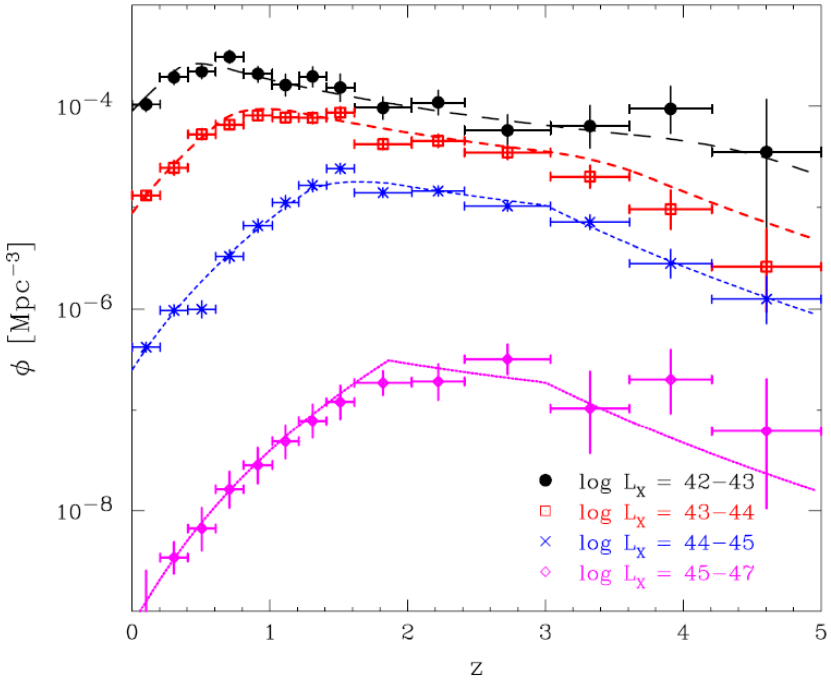

Figure 12. Comoving number density of AGNs plotted against redshift in different luminosity bins (CTN AGNs only). The curves are the best-fit model, and the data points are calculated from either the soft- or hard-band sample (see Section 6).

Ueda, MA et al. 2014

Compton-thick: X-ray “missed”

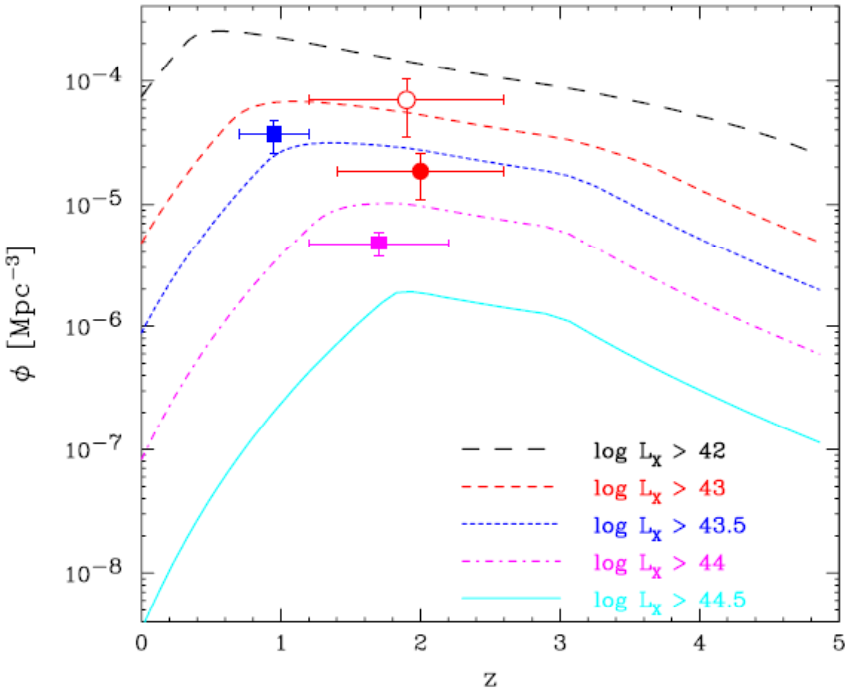

Figure 18. Comoving number density of CTK AGNs with different lower limits for the X-ray luminosity predicted from our baseline model. The data points represent the estimates by Alexander et al. (2011) for log $L_X \gtrsim 43$ (filled circle. red), Fiore et al. (2008) for log $L_X > 43$ (open circle, red), and Fiore et al. (2009) for log $L_X > 43.5$ (filled square, blue) and for log $L_X > 44$ (filled square, magenta).

Targets

- z~1-2 “complete” AGN candidates:
  - BHMF + ERDF + obscuration
  - 10,000 AGNs down to i<23-24, 30 sq.deg. = HSC-Deep
  - In addition to the “galaxy” samples, we need to specifically include “stellar” AGNs in the redshift range.
  - However, selecting (broad-line) AGNs at intermediate redshifts based on the HSC dataset is not an obvious task…
    - Modified KX-method with K-band coverage / Spitzer coverage
    - Availability of U-band deep imaging
    - X-ray + Radio (limited area)
- z~4 AGN candidates:
  - BHMF + ERDF + clustering analysis
  - 10,000 AGNs down to i<23, 100 sq.deg. = HSC-Deep/Wide
  - Pre-selection with HSC photometric dataset

Apparent magnitude distribution of AGNs

- X-ray-selected AGN samples: Blue: broad-line, Red: narrow-line AGNs

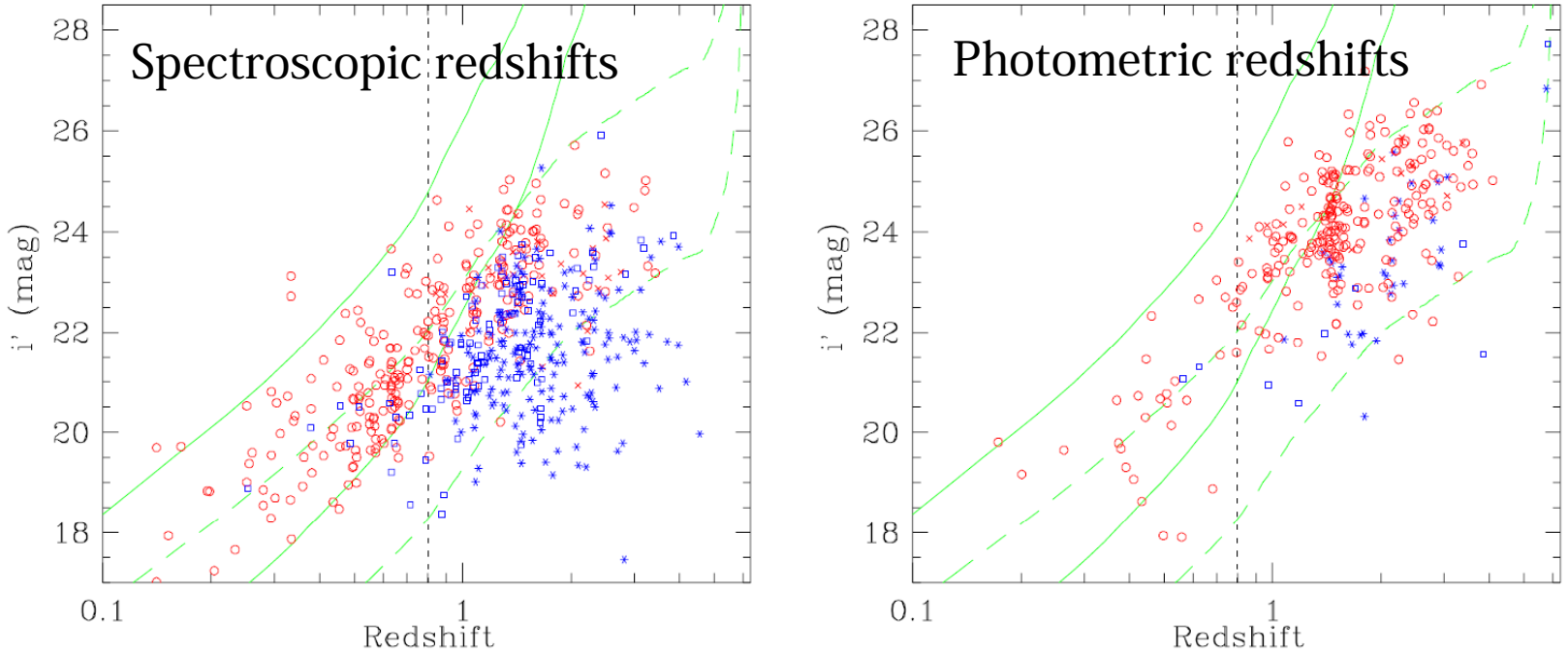

Fig. 10. Left) Stellarity distribution of spectroscopically identified AGNs plotted on the redshift vs. i'-band magnitude plane. Blue asterisks and red crosses represent AGNs with stellar morphology in the i'-band image. Blue (square and asterisk) and red (circle and cross) symbols show broad-line and narrow-line AGNs, respectively. The vertical dotted line marks $z = 0.8$. The green lines indicate the redshift evolution of the i'-band magnitude for a 10Gyr-old (solid) and 2Gyr-old (dashed) single burst stellar population with stellar mass of $\log M_* = 10.5$ (upper) and $\log M_* = 12.0$ (lower). Right) Same for AGNs without spectroscopic identification. In this panel, AGNs are classified photometrically as described in Section 6.2.

Akiyama et al. 2015, PASJ

Importance of spectro-flux calibration

- Spectro-flux calibration is important ! (at leaset overall shape of a spectrum) not only for BH mass estimate, but also for galaxy studies.

3000A continuum to “L”

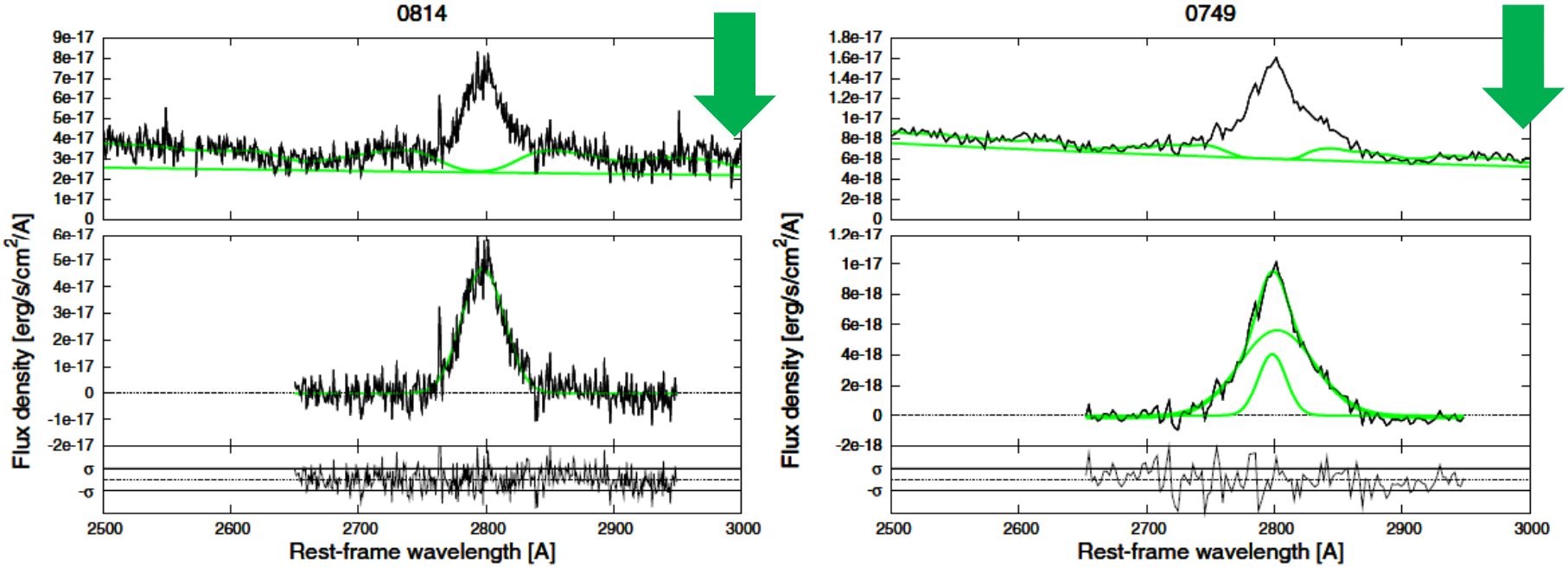

Figure 3. Examples of broad Mg II fitting. Upper panels show the observed data (thin solid line) and the best-fit model from the power-law continuum and Fe II fitting (thick solid line). The power-law component of the best-fit model is also shown separately. The middle panels show the results of the broad Mg II line fitting. The pure Mg II component after subtracting the power-law continuum and Fe II components and the best-fit model from the Mg II fitting are shown with the thin solid line and thick solid line, respectively. Each component of the best-fit model is also shown. Only the wavelength range used for the broad-line fitting is plotted. Bottom panels show the residual after fitting. Left: SXDS0814 with single broad line, and right: SXDS0749 with two components.

Nobuta, MA, et al, 2012, ApJ, 761, 143

KX-QSO selection
for selecting intermediate-z AGN candidates

- QSOs show hot-dust emission as NIR excess above 2 μ m. The “K-band” excess can be used as an indicator of (non-obscured/obscured) AGN activity.

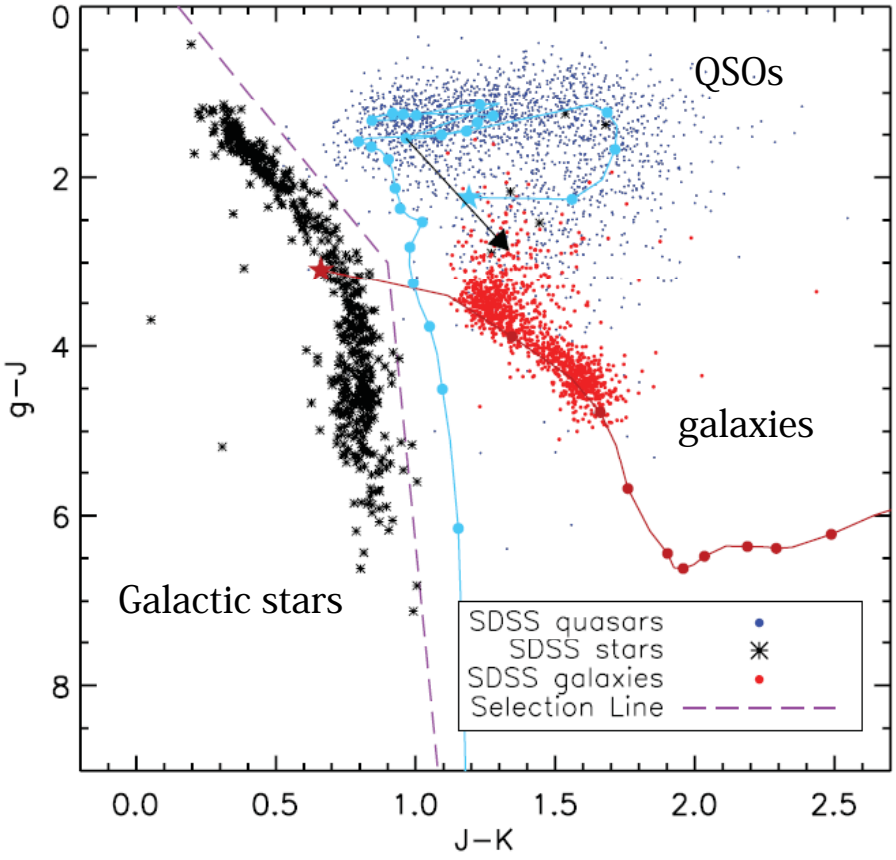

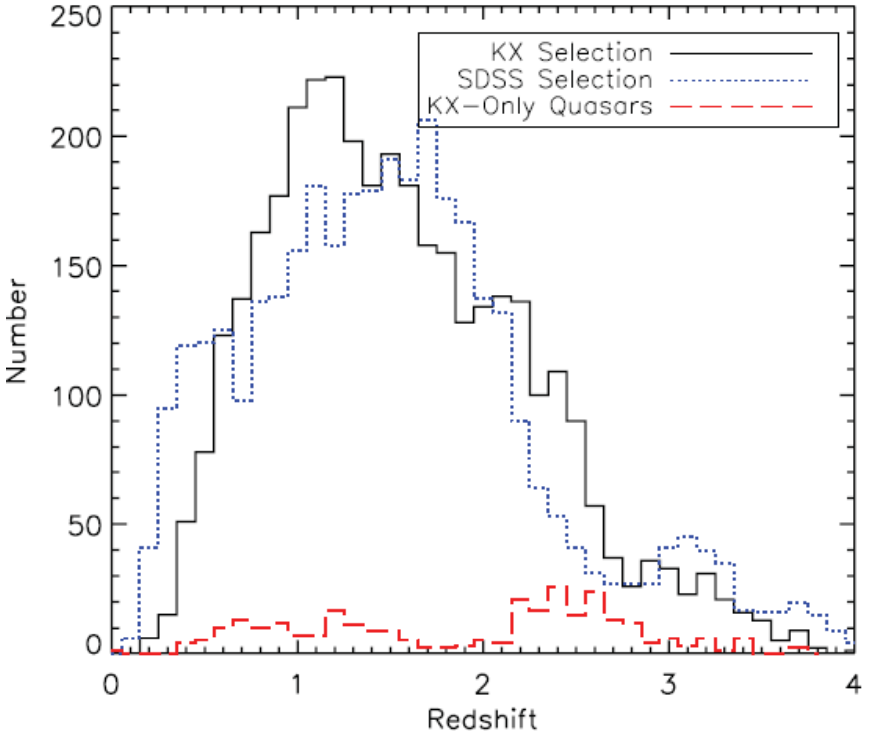

UKIDSS LAS (K=18.3) – SDSS photometry

Magnitudes are in Vega system

Maddox et al. 2012

Modified versions of KX-QSO selection

- X-ray selected AGNs in SXDS (Blue: broad-line AGNs, Red: narrow-line AGNs). Green dots represent non X-ray galaxies. X-ray AGNs overlapping with green dots are dominated by host galaxy emission (faint AGNs/obscured AGNs), and they should be selected with “galaxy”-selection criteria of PSF surveys. In addition to them, we need to add “stellar” KX objects as candidates of broad-line AGNs (objects in cyan and pink regions). We can use y-band photometry instead of J-band in these figures.

UKIDSS DXS depth
K<23.0 objects (stellar, extended)

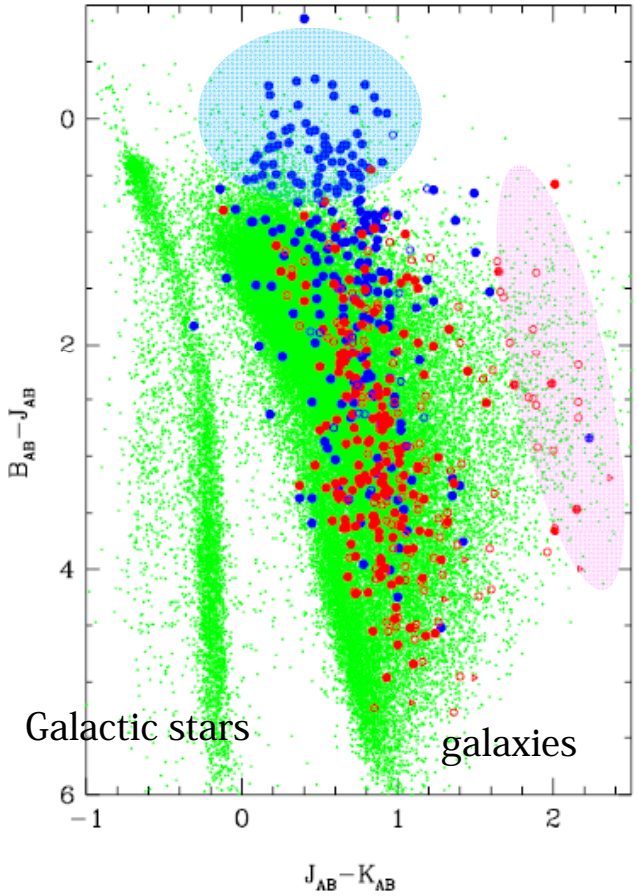

Spitzer SWIRE depth
I1<23.0 objects (stellar, extended)

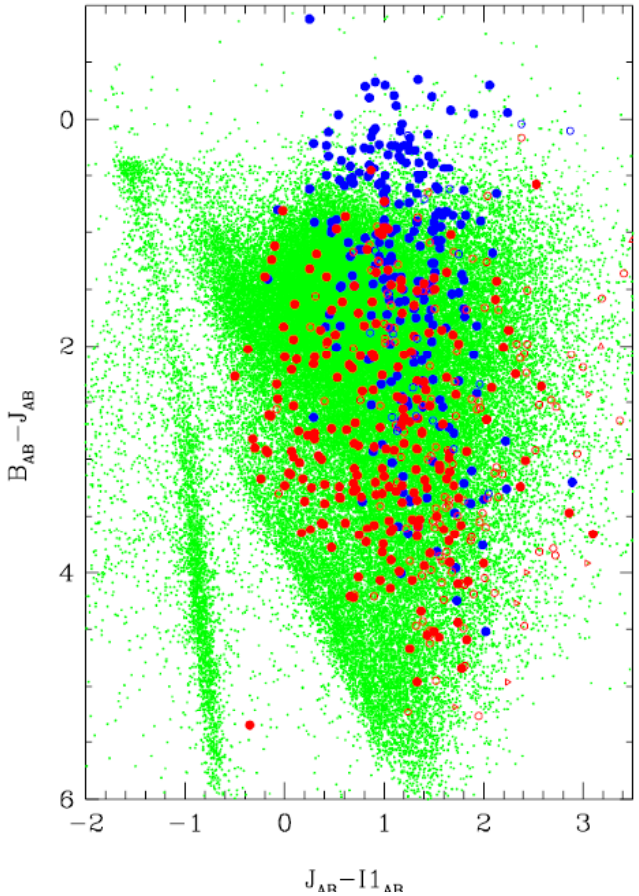

Selecting z~4 AGN candidates

- "Complete" approach is not effective for high-z AGN survey, pre-selection is necessary.
  - 9.1 / degree^2 i<23.0mag
  - 90 / degree^2 i<24.0mag : fraction of contamination needs to be evaluated.

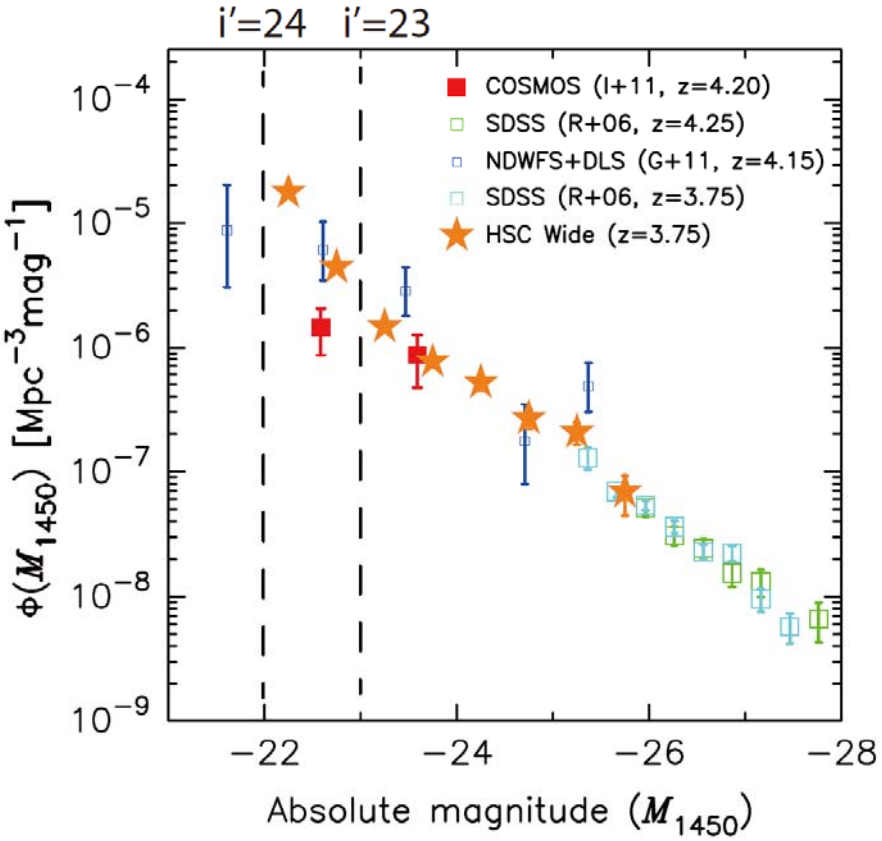

Targets

- z~1-2 “complete” AGN candidates:
  - BHMF + ERDF + obscuration
  - 10,000 AGNs down to i<23-24, 30 sq.deg. = HSC-Deep
  - In addition to the “galaxy” samples, we need to specifically include “stellar” AGNs in the redshift range.
  - However, selecting (broad-line) AGNs at intermediate redshifts based on the HSC dataset is not an obvious task…
    - Modified KX-method with K-band coverage / Spitzer coverage
    - Availability of U-band deep imaging
    - X-ray + Radio (limited area)
- z~4 AGN candidates:
  - BHMF + ERDF + clustering analysis
  - 10,000 AGNs down to i<23, 100 sq.deg. = HSC-Deep/Wide
  - Pre-selection with HSC photometric dataset

Merit of the wide wavelength coverage of PFS

- We can reliably connect measurements in wide redshift range.